

HAN: Higher-order Attention Network for Spoken Language Understanding

Dongsheng Chen, Zhiqi Huang, Yuexian Zou

Peking University, China

chends@stu.pku.edu.cn, {zhiqihuang, zouyx}@pku.edu.cn

Abstract

Spoken Language Understanding (SLU), including intent detection and slot filling, is a core component in human-computer interaction. The natural attributes of the relationship among the two subtasks make higher requirements on fine-grained feature interaction, i.e., the token-level intent features and slot features. Previous works mainly focus on jointly modeling the relationship between the two subtasks with attention-based models, while ignoring the exploration of attention order. In this paper, we propose to replace the conventional attention with our proposed Bilinear attention block and show that the introduced Higher-order Attention Network (HAN) brings improvement for the SLU task. Importantly, we conduct wide analysis to explore the effectiveness brought from the higher-order attention.

1 Introduction

Intent detection (ID) and Slot filling (SF) play important roles in SLU system. For instance, given an utterance "*I want to listen to Hey Jude*", ID can be seen as a classification task to identify the user's intent is to listen to a song and SF can be treated as a sequence labeling task to produce a slot label sequence in BIO format (Ramshaw and Marcus, 1999; Zhang and Wang, 2016) which demonstrate that *Hey Jude* is the song's title. Table 1 shows the expected output of SLU system for this instance.

Taking into account the relationship between these two tasks, joint modeling of them has gradually become the dominant method recently (Goo et al., 2018; Liu et al., 2019b; Niu et al., 2019; Qin et al., 2019, 2020; Huang et al., 2020; Zhou et al., 2020; Huang et al., 2021c). The state-of-the-art methods (Li et al., 2018; Qin et al., 2019, 2020) adopt the attention mechanism (Vaswani et al., 2017) to trigger the mutual interaction between intent features and slot features. Concretely,

Utter.	I	want	to	listen	to	Hey	Jude
Slot	O	O	O	O	O	B-SONG	I-SONG
Intent	PLAY_SONG						

Table 1: Example of SLU output for an utterance. Slot labels are in BIO format: B indicates the start of a slot span, I indicates the inside of a span while O denotes that the word does not belong to any slot.

the attention mechanism learns a set of weights which reflect the importance of different words of an utterance via linearly fusing the given query and key via element-wise sum, and the weights are then applied to the value to derive a weighted sum which represents the enhanced intent or slot representation in a co-interactive way.

In this paper, we argue that the inherent design of conventional attention mechanism can only model the 1st order feature interaction between query and key, which, however, is inefficient to model the relationship between ID and SF. Therefore, to obtain more representative intent and slot features, we propose to exploit higher-order interactions from 2nd order feature interaction via bilinear pooling, which is an operation to calculate outer product between two feature vectors. Such technique can enable the 2nd order feature interaction by taking all pair-wise interactions between query and key into account and thus provide more discriminative representations. Lin et al. (2015) first applied bilinear pooling to fuse visual features for fine-grained visual recognition. In order to mitigate the high computational complexity of bilinear pooling, Kim et al. (2016) proposed low-rank bilinear pooling with linear mapping and Hadamard product. Inspired by the successful application of bilinear pooling in the field of Computer Vision research, we proposed our BiLinear attention block as shown in Figure 1, which can build the 2nd order interactions between intent and slot features and get more discriminative intent and slot representations. Intuitively, a stack of the blocks is readily grouped to go beyond bilinear models and extract higher-order interactions.

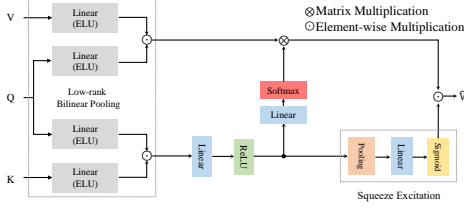


Figure 1: The proposed BiLinear attention block, which is based on the low-rank bilinear pooling (Kim et al., 2016).

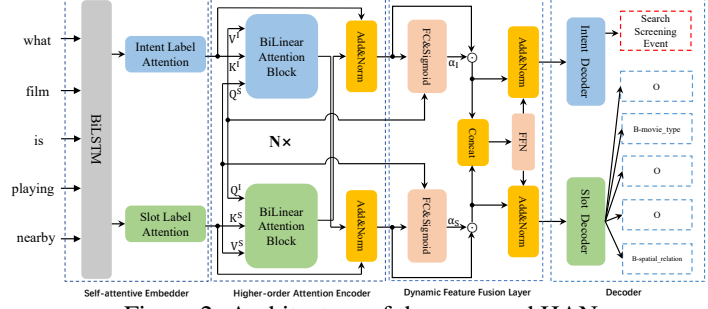


Figure 2: Architecture of the proposed HAN.

To this end, we also provide the view of how to integrate such blocks into HAN for building higher-order feature interactions. The experiments show that our model achieves new state-of-the-art results on two benchmark datasets SNIPS (Coucke et al., 2018) and ATIS (Hemphill et al., 1990).

2 Approach

We briefly formulate our HAN (Figure 2) which consists of four parts and introduce our BiLinear attention block in detail.

2.1 BiLinear attention block

In this section, we will describe the proposed Bilinear attention block as shown in Figure 1 in detail.

Supposed we have a query $\mathbf{q} \in \mathbb{R}^d$, a set of keys $\mathbf{K} = \{\mathbf{k}_i\}_{i=1}^n$, and a set of values $\mathbf{V} = \{\mathbf{v}_i\}_{i=1}^n$, where $\mathbf{k}_i, \mathbf{v}_i \in \mathbb{R}^d$ denote the i -th key/value pair. Our block first performs low-rank bilinear pooling (Kim et al., 2016) to achieve a joint bilinear query-key representation $\mathbf{B}_i^k \in \mathbb{R}^d$ to model the 2^{nd} order feature interactions between query and key: $\mathbf{B}_i^k = \text{ReLU}(\mathbf{W}_k \mathbf{k}_i) \odot \text{ReLU}(\mathbf{W}_q^k \mathbf{q})$, where $\mathbf{W}_k, \mathbf{W}_q^k \in \mathbb{R}^{d \times d}$ are weight matrices.

Next, depending on all bilinear query-key representations $\{\mathbf{B}_i^k\}_{i=1}^n$, two kinds of bilinear attention distributions are obtained to aggregate both contextual and channel-wise information within all values. Specifically, the contextual bilinear attention distribution is introduced by projecting each bilinear query-key representation into the corresponding attention weight via two embedding layers, followed with a softmax layer for normalization:

$$\begin{aligned} \mathbf{B}_i^{\prime k} &= \text{ReLU}(\mathbf{W}_B^k \mathbf{B}_i^k); b_i^s = \mathbf{W}_b \mathbf{B}_i^{\prime k}; \\ \beta_i^s &= \text{softmax}(\mathbf{b}^s), \end{aligned} \quad (1)$$

where $\mathbf{W}_B^k \in \mathbb{R}^{d \times d}$ and $\mathbf{W}_b \in \mathbb{R}^{1 \times d}$ are weight matrices, $\mathbf{B}_i^{\prime k}$ is the transformed bilinear query-key representation, and b_i^s is the i -th element in \mathbf{b}^s . Here each element β_i^s in β^s denotes the normalized

contextual attention weight for each key/value pair. Meanwhile, we perform a squeeze-excitation operation over all transformed bilinear query-key representations $\{\mathbf{B}_i^{\prime k}\}_{i=1}^n$ for channel-wise attention measurement. Concretely, the operation of squeeze aggregates all transformed bilinear query-key representations via average pooling, leading to a global channel descriptor $\bar{\mathbf{B}} = \frac{1}{n} \sum_{i=1}^n \mathbf{B}_i^{\prime k}$. After that, the followed excitation operation produces channel-wise attention distribution β^c by leveraging the self-gating mechanism with a sigmoid over the $\bar{\mathbf{B}}$:

$$\mathbf{b}^c = \mathbf{W}_e \bar{\mathbf{B}}, \beta^c = \sigma(\mathbf{b}^c), \quad (2)$$

where $\mathbf{W}_e \in \mathbb{R}^{d \times d}$ is weight matrix.

Finally, our BiLinear attention block generates the attended value feature $\hat{\mathbf{v}}_i$ by accumulating the enhanced bilinear values with contextual and channel-wise bilinear attention:

$$\hat{\mathbf{v}}_i = \beta^c \odot \sum_{i=1}^n \beta_i^s \mathbf{B}_i^v, \quad (3)$$

$$\mathbf{B}_i^v = \text{ReLU}(\mathbf{W}_v \mathbf{v}_i) \odot \text{ReLU}(\mathbf{W}_q^v \mathbf{q}_i),$$

where \mathbf{B}_i^v denotes the enhanced value of bilinear pooling on query \mathbf{q}_i and each value \mathbf{v}_i , $\mathbf{W}_v \in \mathbb{R}^{d \times d}$ and $\mathbf{W}_q^v \in \mathbb{R}^{d \times d}$ are weight matrices. As such, BiLinear attention block produces more representative attended feature since higher-order feature interactions are exploited via bilinear pooling. We iterate the above process n times with $\mathbf{Q} = \{\mathbf{q}_i\}_{i=1}^n$, and get a set of values $\hat{\mathbf{V}} = \{\hat{\mathbf{v}}_i\}_{i=1}^n$:

$$\hat{\mathbf{V}} = F_{BiLinear}(\mathbf{K}, \mathbf{V}, \mathbf{Q}), \quad (4)$$

where $\hat{\mathbf{V}} \in \mathbb{R}^{n \times d}$ is the enhanced features with higher-order attention feature interactions. By equipping the block with *Exponential Linear Unit (ELU)* (Barron, 2017), it can model infinity order feature interactions, which can be proved via Taylor expansion of each element in bilinear vector after

Model	SNIPS			ATIS		
	Slot (F1)	Intent (Acc)	Overall (Acc)	Slot (F1)	Intent (Acc)	Overall (Acc)
Stack-Propagation (Qin et al., 2019)	94.20	98.00	86.90	95.90	96.90	86.50
Co-Interactive (Qin et al., 2020)	95.35	98.71	89.12	95.47	97.65	86.69
Graph-LSTM (Zhang et al., 2020)	95.30	98.29	89.71	95.91	97.20	87.57
Baseline (BiLSTM+Decoder)	94.19	97.79	85.86	95.32	95.63	84.99
+ (Label attention+shallow concat)	94.39	98.03	87.89	95.55	97.52	85.89
+ Conventional Attention (1^{st} order based model)	95.37	98.34	88.12	95.64	97.43	87.01
+ Bilinear attention block	95.35	98.43	88.57	95.83	97.43	87.32
+ Dynamic Feature Fusion	95.57	98.57	89.43	95.88	97.56	87.57
+ ELU	96.01	98.69	90.43	95.95	97.89	88.12
HAN (Ours)	96.18	99.12	91.80	96.12	98.04	88.47
HAN w/ BERT	97.66	99.23	93.54	96.83	98.54	89.31

Table 2: Performance of different model on the SNIPS and ATIS datasets. Our HAN achieves the state-of-the-art performance on the two benchmark datasets.

exponential transformation. Specifically, for two vectors X and Y , their exponential bilinear pooling can be estimated using the Taylor expansion:

$$\begin{aligned}
& \exp(W_X X) \odot \exp(W_Y Y) \\
&= [\exp(W_X^1 X) \odot \exp(W_Y^1 Y), \dots, \exp(W_X^D X) \odot \exp(W_Y^D Y)] \\
&= [\exp(W_X^1 X + W_Y^1 Y), \dots, \exp(W_X^D X + W_Y^D Y)] \\
&= \left[\sum_{p=0}^{\infty} \gamma_p^1 (W_X^1 X + W_Y^1 Y)^p, \dots, \sum_{p=0}^{\infty} \gamma_p^D (W_X^D X + W_Y^D Y)^p \right],
\end{aligned}$$

where W_X and W_Y are embedding matrices, D denotes the dimension of bilinear vector, W_X^i/W_Y^i is the i -th row in W_X/W_Y .

2.2 Overview of the HAN

Self-attentive Embedder Inspired by Qin et al. (2019), we employ the Self-attentive Embedder to obtain the utterance embeddings. It first uses a shared BiLSTM to embed the input sequence, acquiring $\mathbf{H} = (\mathbf{h}_1, \mathbf{h}_2, \dots, \mathbf{h}_n)$. Then, it perform the label attention (Cui and Zhang, 2019) over intent and slot label to get the explicit intent and slot representation $\mathbf{H}_I \in \mathbb{R}^{n \times d}$, $\mathbf{H}_S \in \mathbb{R}^{n \times d}$ ($d = 128$), which capture the intent and slot semantic information, respectively.

Higher-order Attention Encoder \mathbf{H}_I and \mathbf{H}_S are further fed into the our Higher-order Attention Encoder to strengthen both the intent and slot features via capturing higher-order feature interactions between them. Formally, the encoder is composed of a stack of $N = 2$ identical sublayers. Each sublayer is our Bilinear attention block, followed by layer normalization. Same with Vaswani et al. (2017), we first map the matrix \mathbf{H}_I and \mathbf{H}_S to queries($\mathbf{Q}_I^{(1)}, \mathbf{Q}_S^{(1)}$), keys($\mathbf{K}_I^{(1)}, \mathbf{K}_S^{(1)}$) and values($\mathbf{V}_I^{(1)}, \mathbf{V}_S^{(1)}$) matrices by using different linear projections. Then we take $\mathbf{Q}_I^{(1)}, \mathbf{K}_S^{(1)}$ and $\mathbf{V}_S^{(1)}$ as queries, keys and values, respectively,

acquiring the enhanced values:

$$\begin{aligned}
\mathbf{V}_I^{(1)} &= F_{BiLinear}(\mathbf{K}_S^{(1)}, \mathbf{V}_S^{(1)}, \mathbf{Q}_I^{(1)}), \\
\mathbf{H}_I^{(1)} &= \text{LN}(\mathbf{H}_I + \mathbf{V}_I^{(1)}),
\end{aligned} \tag{5}$$

where LN represents the layer normalization (Ba et al., 2016). Similarly, we take $\mathbf{Q}_S^{(1)}$ as queries, $\mathbf{K}_I^{(1)}$ as keys and $\mathbf{V}_I^{(1)}$ as values to obtain $\mathbf{H}_S^{(1)}$.

After repeating N times, we can obtain the enhanced intent features $\mathbf{H}_I^{(N)} \in \mathbb{R}^{n \times d}$ and slot features $\mathbf{H}_S^{(N)} \in \mathbb{R}^{n \times d}$, which are endowed with the higher-order feature interactions in between.

Dynamic Feature Fusion Layer We first compute two weight matrices α_I and α_S which reflect the relevance between the output and the input query of the last sublayer in the Higher-order Attention Encoder, and thus obtain the fused features \mathbf{H}_{IS} , which can be defined as follows:

$$\begin{aligned}
\alpha_I &= \sigma(W_I[\mathbf{Q}_I^{(N)}, \mathbf{H}_I^{(N)}] + b_I), \\
\alpha_S &= \sigma(W_S[\mathbf{Q}_S^{(N)}, \mathbf{H}_S^{(N)}] + b_S), \\
\mathbf{H}_{IS} &= \alpha_I \odot \mathbf{H}_I^{(N)} \oplus \alpha_S \odot \mathbf{H}_S^{(N)},
\end{aligned} \tag{6}$$

where $[\cdot, \cdot]$ indicates concatenation, σ is the sigmoid activation; \odot denotes element-wise multiplication; W_I and W_S are both $2d \times d$ embedding matrices, b_I and b_S are biases. Then, we adopt the feed-forward network (FFN) (Zhang and Wang, 2016), to acquire the updated intent features $\hat{\mathbf{H}}_I^{(N)} \in \mathbb{R}^{n \times d}$ and slot features $\hat{\mathbf{H}}_S^{(N)} \in \mathbb{R}^{n \times d}$, i.e., $\hat{\mathbf{H}}_I^{(N)} = \text{LN}(\text{FFN}(\mathbf{H}_{IS}) + \mathbf{H}_I^{(N)})$ and $\hat{\mathbf{H}}_S^{(N)} = \text{LN}(\text{FFN}(\mathbf{H}_{IS}) + \mathbf{H}_S^{(N)})$.

SLU Decoder For the intent detection, we follow Kim (2014) to employ the *maxpooling* on $\hat{\mathbf{H}}_I^{(N)}$ to obtain \mathbf{c} , which is used to predict the intent label: $\mathbf{o}^I \sim \hat{\mathbf{y}}^I = \text{softmax}(\mathbf{W}^I \mathbf{c} + \mathbf{b}_I)$,

For the slot filling, we apply a standard CRF layer (Niu et al., 2019) to model the dependency

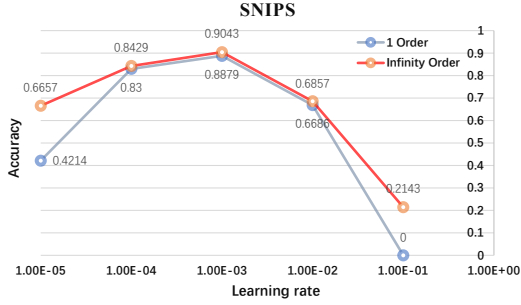


Figure 3: Performance of the SLU model w/ ELU (HAN) and w/o ELU (1st order) under different learning rate. The 1st order based model is acquired by replacing our higher-order attention with the conventional attention model (Vaswani et al., 2017).

between labels, and then predict the label sequence $P(\hat{y}|\mathbf{O}_S) = \frac{\sum_{i=1} \exp f(y_{i-1}, y_i, \mathbf{O}_S)}{\sum_{y'} \sum_{i=1} \exp f(y'_{i-1}, y'_i, \mathbf{O}_S)}$, where $f(y'_{i-1}, y'_i, \mathbf{O}_S)$ computes the transition score from y_{i-1} to y_i and $\mathbf{O}_S = \mathbf{W}^S \mathbf{H}_S^{(N)} + \mathbf{b}_S$.

3 Experiments

Main Results Table 2 shows the results of our approach on the SNIPS and ATIS, our HAN outperforms all baselines and achieves the state-of-the-art performance. Besides, fine-tuned with the strong pre-trained language model (BERT) (Devlin et al., 2019), HAN has been further improved. For the ablation study, we can see that as adding each key component of the model gradually, the performance gradually becomes better, and it gets improvement when equipping with ELU (4.57% and 3.13% improvement compared to baseline in overall accuracy on the SNIPS and ATIS dataset, respectively). The "shallow concat" means directly concatenate the two features without dynamic feature fusion mentioned above.

Robustness towards Learning Rate From Figure 3, with the overall Accuracy as metric, we show that under same experimental settings, infinity order SLU model performs better than the first order model under different learning rate. Besides, we find that under reasonable and task-specific range of the learning rate, i.e., 1e-4 to 1e-2, the higher-order based model performs slightly and consistently better than the 1st order based model. While when the learning rate is out of this range, i.e., bigger than 1e-2 or smaller than 1e-4, the performance of the 1st order based model occurs to crack down quickly and it even drops to 0 when the learning rate is 0.1. Oppositely, the higher-order based

Model	HAE	SNIPS			ATIS		
		Slot	Intent	Overall	Slot	Intent	Overall
Stack-Propagation (Qin et al., 2019)	×	94.20	98.00	86.90	95.90	96.90	86.50
	✓	94.70	98.20	87.20	96.20	97.50	87.40
Co-Interactive (Qin et al., 2020)	×	95.35	98.71	89.12	95.47	97.65	86.69
	✓	95.49	98.57	89.86	95.98	97.87	87.35
HAN (Ours)	×	95.43	98.57	89.29	95.87	97.42	87.12
	✓	96.18	99.12	91.80	96.12	98.04	88.47

Table 3: Impact of higher-order attention on different baselines, i.e., Stack Propagation, Co-Interactive, and our HAN.

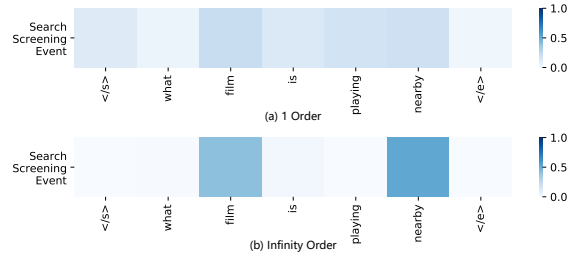


Figure 4: Visualization of our proposed methods. The utterance is acquired from the SNIPS dataset.

model, though also drops down when the learning reaches is set out of reasonable range, can still keep considerable performance compared to the first order base model, and thus shows its robustness to the extreme case towards the optimized learning rate. A similar phenomenon also can be found on the ATIS dataset (please see our Appendix).

Generalization Analysis We attempt to incorporate the Higher-order Attention Encoder (marked as HAE) into several existing baselines. Table 3 shows that baselines with infinity order attention, i.e., HAE, performs better than it with 1st order attention model in most of the case. This further verifies the generalization of the effectiveness of the higher-order attention on the SLU task.

Visualization of the Infinity Order Attention To explore the model promotion brought from the proposed HAN, we turn to visualize the attention pattern over Q and K in Eq. (5). As can be seen in Figure 4, where we use the utterance "What film is playing nearby" from the SNIPS dataset, the proposed higher-order attention model shows clearer attention capture ability compared to the original 1st attention mechanism, it can better focus on the keyword *film* and *nearby*.

4 Conclusion

In this paper, we propose a novel Bilinear attention block which can build the 2nd order interactions between intent and slot features and get more dis-

criminative intent and slot representations. The higher and even infinity order feature interactions can be readily modeled via stacking multiple Bi-Linear attention blocks and equipping the block with ELU activation. Moreover, we introduced the HAN, and conducted numerous experiments and analysis on SNIPS and ATIS datasets to demonstrate the effectiveness of our method.

A Related Work

A.1 Spoken Language Understanding

Spoken Language Understanding is a well known task in dialogue system, and it typically contains intent detection and slot filling tasks. The special relation of the two tasks requires them to have enough correlation and interaction, making it possible to explore the promotion brought from higher order attention.

A.2 Bilinear Pooling

Bilinear pooling was first proposed in (Lin et al., 2015) to fuse the features for fine-grained visual recognition, it can provide 2^{nd} order interaction on feature vectors. Later for the SLU task, Teng et al. (2020) proposed to use Bilinear pooling to fuse the word information and character information, showing that such method can provide more discriminative representations than simple pooling, i.e., 1^{st} order, for the spoken language understanding task.

B Experimental Details

B.1 Experimental Settings

We adopt the RAdam (Liu et al., 2019a) optimizer for optimizing the parameters, with a mini-batch size of 32 and initial learning rate of 0.001. We use 300d GloVe pre-trained vector (Pennington et al., 2014) as the initialization embedding. The hidden dimensionality is set as 128. Two evaluation metrics are used in the SLU task. The performance of intent detection is measured by accuracy, while slot filling is evaluated with the F1 score, and the sentence-level semantic frame parsing using overall accuracy.

C More Experiment Results

C.1 Learning Rate on ATIS

Besides the performance of the higher order model and the first order model in the SNIPS dataset w.r.t, learning rate in Section 3, we also show the results

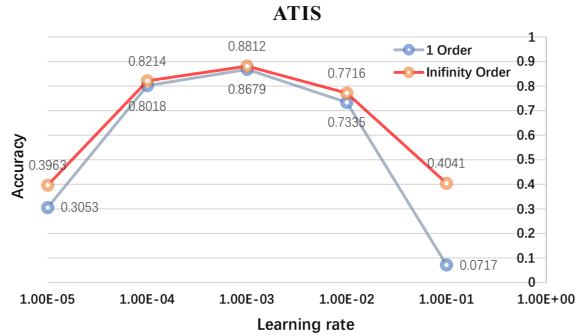


Figure 5: Performance of the model w/ELU and wo/ELU under different learning rate on the ATIS dataset.

L	ELU	SNIPS			ATIS		
		Slot	Intent	Overall	Slot	Intent	Overall
1	×	95.57	98.57	89.43	95.88	97.56	87.57
	✓	96.01	98.69	90.43	95.95	97.89	88.12
2	×	95.86	98.57	89.71	95.92	97.76	87.79
	✓	96.18	99.12	91.80	96.12	98.04	88.47
3	×	95.65	98.29	89.57	95.75	97.54	87.12
	✓	95.70	98.57	89.86	95.75	97.42	87.23
4	×	95.51	98.00	89.00	95.75	97.31	87.01
	✓	95.65	98.29	89.11	95.77	97.42	87.01
5	×	95.12	97.86	88.86	95.58	97.54	86.67
	✓	95.32	98.14	88.86	95.83	97.31	86.90

Table 4: Comparison of different order model.

in the ATIS dataset. From Figure 5, we can see that the higher order attention based model performs better than the first order based model consistently, and it shows a clear robustness towards the learning rate for its adaptive capacity in the hyper-parameter.

C.2 Discussion on the layer number of Higher-order Attention Encoder

From Table 4, we can see that when the number of sublayers in Higher-order Attention Encoder is 2, performance of HAN on both validation dataset gets the best. So we set the number of sublayers $N = 2$. We speculate that the increased parameters by stacking more blocks might result in overfitting, which somewhat hinders the exploitation of higher order interaction in this way.

References

Jimmy Lei Ba, Jamie Ryan Kiros, and Geoffrey E Hinton. 2016. Layer normalization. *arXiv preprint arXiv:1607.06450*.

- Jonathan T Barron. 2017. Continuously differentiable exponential linear units. *arXiv preprint arXiv:1704.07483*.
- Alice Coucke, Alaa Saade, Adrien Ball, Théodore Bluche, Alexandre Caulier, David Leroy, Clément Doumouro, Thibault Gisselbrecht, Francesco Caltagirone, Thibaut Lavril, Maël Primet, and Joseph Dureau. 2018. Snips voice platform: an embedded spoken language understanding system for private-by-design voice interfaces. *CoRR*, abs/1805.10190.
- Leyang Cui and Yue Zhang. 2019. Hierarchically-refined label attention network for sequence labeling. *arXiv preprint arXiv:1908.08676*.
- Jacob Devlin, Ming-Wei Chang, Kenton Lee, and Kristina Toutanova. 2019. BERT: pre-training of deep bidirectional transformers for language understanding. In *NAACL-HLT*.
- Chih-Wen Goo, Guang Gao, Yun-Kai Hsu, Chih-Li Huo, Tsung-Chieh Chen, Keng-Wei Hsu, and Yun-Nung Chen. 2018. Slot-gated modeling for joint slot filling and intent prediction. In *Proceedings of the 2018 Conference of the North American Chapter of the Association for Computational Linguistics*.
- Charles T Hemphill, John J Godfrey, and George R Doddington. 1990. The atis spoken language systems pilot corpus. In *Speech and Natural Language*.
- Lu Hou, Zhiqi Huang, Lifeng Shang, Xin Jiang, Xiao Chen, and Qun Liu. 2020. Dynabert: Dynamic BERT with adaptive width and depth. In *NeurIPS*.
- Zhiqi Huang, Lu Hou, Lifeng Shang, Xin Jiang, Xiao Chen, and Qun Liu. 2021a. Ghostbert: Generate more features with cheap operations for BERT. In *ACL/IJCNLP*.
- Zhiqi Huang, Fenglin Liu, Xian Wu, Shen Ge, Helin Wang, Wei Fan, and Yuexian Zou. 2021b. Audio-oriented multimodal machine comprehension via dynamic inter- and intra-modality attention. In *AAAI*.
- Zhiqi Huang, Fenglin Liu, Peilin Zhou, and Yuexian Zou. 2021c. Sentiment injected iteratively co-interactive network for spoken language understanding. In *ICASSP*.
- Zhiqi Huang, Fenglin Liu, and Yuexian Zou. 2020. Federated learning for spoken language understanding. In *COLING*. International Committee on Computational Linguistics.
- Jin-Hwa Kim, Kyoung-Woon On, Woosang Lim, Jeonghee Kim, Jung-Woo Ha, and Byoung-Tak Zhang. 2016. Hadamard product for low-rank bilinear pooling. *arXiv preprint arXiv:1610.04325*.
- Yoon Kim. 2014. Convolutional neural networks for sentence classification. In *EMNLP*.
- Changliang Li, Liang Li, and Ji Qi. 2018. A self-attentive model with gate mechanism for spoken language understanding. In *EMNLP*.
- Tsung-Yu Lin, Aruni RoyChowdhury, and Subhransu Maji. 2015. Bilinear CNN models for fine-grained visual recognition. In *ICCV*.
- Liyuan Liu, Haoming Jiang, Pengcheng He, Weizhu Chen, Xiaodong Liu, Jianfeng Gao, and Jiawei Han. 2019a. On the variance of the adaptive learning rate and beyond. *arXiv preprint arXiv:1908.03265*.
- Yijin Liu, Fandong Meng, Jinchao Zhang, Jie Zhou, Yufeng Chen, and Jinan Xu. 2019b. Cm-net: A novel collaborative memory network for spoken language understanding. *arXiv preprint arXiv:1909.06937*.
- Peiqing Niu, Zhongfu Chen, Meina Song, et al. 2019. A novel bi-directional interrelated model for joint intent detection and slot filling. *arXiv preprint arXiv:1907.00390*.
- Jeffrey Pennington, Richard Socher, and Christopher D Manning. 2014. Glove: Global vectors for word representation. In *Proceedings of the 2014 conference on empirical methods in natural language processing (EMNLP)*, pages 1532–1543.
- Libo Qin, Wanxiang Che, Yangming Li, Haoyang Wen, and Ting Liu. 2019. A stack-propagation framework with token-level intent detection for spoken language understanding. *arXiv preprint arXiv:1909.02188*.
- Libo Qin, Tailu Liu, Wanxiang Che, Bingbing Kang, Sendong Zhao, and Ting Liu. 2020. A co-interactive transformer for joint slot filling and intent detection. *arXiv preprint arXiv:2010.03880*.
- Lance A Ramshaw and Mitchell P Marcus. 1999. Text chunking using transformation-based learning. In *Natural language processing using very large corpora*, pages 157–176. Springer.
- Dechuang Teng, Libo Qin, Wanxiang Che, Sendong Zhao, and Ting Liu. 2020. Injecting word information with multi-level word adapter for chinese spoken language understanding. *CoRR*, abs/2010.03903.
- Ashish Vaswani, Noam Shazeer, Niki Parmar, Jakob Uszkoreit, Llion Jones, Aidan N Gomez, Lukasz Kaiser, and Illia Polosukhin. 2017. Attention is all you need. *arXiv preprint arXiv:1706.03762*.
- Linhao Zhang, Dehong Ma, Xiaodong Zhang, Xiaohui Yan, and Houfeng Wang. 2020. Graph lstm with context-gated mechanism for spoken language understanding. In *AAAI*.
- Xiaodong Zhang and Houfeng Wang. 2016. A joint model of intent determination and slot filling for spoken language understanding. In *IJCAI*, volume 16, pages 2993–2999.
- Peilin Zhou, Zhiqi Huang, Fenglin Liu, and Yuexian Zou. 2020. Pin: A novel parallel interactive network for spoken language understanding. *ArXiv*.